Effect of Weld Location, Orientation, and Strain Path on Forming Behavior of AHSS Tailor Welded Blanks

S. K. Panda[1]
Department of Mechanical Engineering,
Indian Institute of Technology,
Kharagpur 721302, India
e-mail: sushanta.panda@mech.iitkgp.ernet.in

J. Li
Department of Mechanical and Mechatronics Engineering,
Centre for Advanced Materials Joining,
University of Waterloo,
Waterloo, ON, N2L3G1, Canada

V. H. Baltazar Hernandez
Department of Mechanical and Mechatronics Engineering,
Centre for Advanced Materials Joining,
University of Waterloo,
Waterloo, ON, N2L3G1, Canada;
MPyM-EPMM Academic Unit of Engineering,
Autonomous University of Zacatecas,
Zacatecas 98000, Mexico

Y. Zhou
Department of Mechanical and Mechatronics Engineering,
Centre for Advanced Materials Joining,
University of Waterloo,
Waterloo, ON, N2L3G1, Canada

F. Goodwin
International Zinc Association,
Durham, NC 27713

Use of multiple advanced high strength steel sheets for fabrication of tailor welded blanks (TWBs) is one of the current interests for automotive and steel industries as it reduces manufacturing cost and weight of the vehicle, and also improves the quality of the component. As the varieties of TWB applications are increasing, the effects of the difference in material properties, weld, and its orientation on blank formability have become important both in deep drawing and stretch forming. In this work, high strength low alloy (HSLA) grade steels were laser welded with two different dual phase steels having 980 MPa (DP980) and 600 MPa (DP600) tensile strengths to fabricate two different material combination TWBs (DP980-HSLA and DP600-HSLA). Formability of these two types of TWBs has been studied experimentally both in biaxial and plane strain stretch forming modes by performing limiting dome height (LDH) tests using a 101.6 mm diameter hemispherical punch. Five different weld locations during biaxial-stretch forming mode, and the effect of weld orientation with respect to major principal strain in plane strain stretch forming mode, have been studied. It was found that formability LDH and failure location depended on weld location, and LDH increased when weld line was positioned at the extreme positions away from the center due to more uniform strain distribution on the deformed dome. The welded blanks had lower formability in plane strain deformation mode compared with biaxial-stretch forming mode. However, influence of weld orientation on the formability depended on material combination. Changes in the fracture mode were confirmed from fractography analysis of biaxial, transverse plane strain, and longitudinal plane strain stretch formed samples.
[DOI: 10.1115/1.4001965]

Keywords: tailor welded blank, advanced high strength steel, formability, stretch forming

1 Introduction

Tailor welded blanks (TWBs) are generally laser welded multiple sheet metals of different strengths, thicknesses, and/or shapes and are then stamped into various final three dimensional desired parts. Along with strength and thickness, forming qualities (such as drawability, stretchability, and springback) and coating characteristics are optimized with properties tailored to fit a particular application. The TWBs offer several notable benefits including reduced manufacturing costs, minimized offal, and improved dimensional consistency [1]. Advanced high strength steels (AHSSs) are multiphase steels. They are manufactured with an intercritical annealing step designed to produce a ferrite and an austenite bimodal microstructure, which upon cooling results in a ferritic matrix with dispersed decomposition products such as martensite and bainite and in some cases, retained austenite [2]. One type, dual phase (DP) steels from the AHSS family have superior combination of strength and formability while being reasonably simple and inexpensive to manufacture. These steels can be considered for potential TWB applications in various body-in-white structures to further reduce weight and improve occupant protection.

Many factors such as mechanical and metallurgical properties of the blank (sheet metal), lubrication, press speed, blank holder pressure, punch, and die design contribute to the success or failure of the stamping to varying degrees in an interdependent manner [3]. However, the forming behavior of a TWB is influenced by many additional factors, such as material property changes in the fusion zone (FZ) and heat-affected zone (HAZ) [4,5]; the effects of the weldment on the strain distribution, failure site, and fracture propagation [6]; and the nonuniform deformation because of the difference in thickness, properties, and/or surface characteristics [7,8]. During sheet metal forming processes, different automotive parts undergo different forming modes (often referred to as strain path) depending on interaction of different tooling design and process design variables. For example, plane strain deformation path is followed while manufacturing trunk lid and roof, whereas biaxial strain path is followed while manufacturing the front door and front fender of an automotive car, as shown in Fig. 1 [9]. Therefore, an effective formability characterization of a TWB should be done by conducting forming test with different strain paths (e.g., uniaxial tensile, plane strain, and biaxial strain path). It will help sheet metal practitioner by providing useful information for correcting failure prior to actual manufacturing of different TWB components.

Reduction in formability as a result of the welding process has been reported for DP980 and DP800 steels [10]. These DP steels have inherently higher alloying levels; as a result, it exhibits high hardenability in the weld fusion zone. Also, exposure to subcritical temperatures in the HAZ causes tempering of martensite phase, resulting in local softening of the microstructure [11].

[1]Corresponding author.

Contributed by the Materials Division of ASME for publication in the JOURNAL OF ENGINEERING MATERIALS AND TECHNOLOGY. Manuscript received January 8, 2010; final manuscript received May 21, 2010; published online September 8, 2010. Assoc. Editor: Yanyao Jiang.

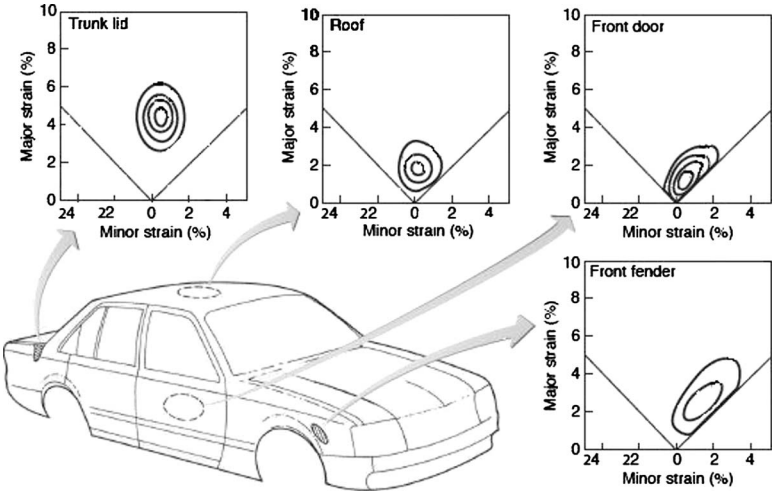

Fig. 1 Major and minor strains (strain path) while stamping various automotive parts

Hence, a high property gradient was found in the weldment of these DP steels, which reduced formability compared with the parent metal [4,5,10]. It was reported that when HSLA was laser welded with DP980 or DP800 steel sheets and biaxially stretch formed during limiting dome height testing, the fracture location shifts from the HAZ soft zone at DP side to the HSLA side [12]. But the formability in terms of limiting dome height (LDH) decreased due to significant difference in properties among both parent metals. All these above mentioned LDH tests were conducted in biaxial-stretch forming mode by keeping the TWBs on the lower die with the weld positioned at the middle of the die opening. In order to take full advantage of the benefits of AHSS and TWB technology, designers need to understand the effect of difference in material properties, weld location, weld orientation, and forming mode (strain path) on formability early in the design process. However, there is no open literature available for understanding the formability of dissimilar TWB combinations comprehensively.

In the present work, two different dissimilar material combinations were fabricated by diode laser welding, and formability of these welded blanks was evaluated through different strain paths (e.g., biaxial strain, plane strain, and uniaxial tensile strain path) by conducting LDH and uniaxial tensile tests. Five different weld locations and two different weld orientations were chosen to understand their influences on forming behavior. Strain distributions on the deformed welded samples were measured and fracture mode was observed to understand the influences of weld location, weld orientation, and strain path.

2 Base Materials and Laser Welded Blank Fabrication

In the present study, three different sheet metals were chosen for TWB fabrication and they are HSLA (high strength steel-HSS), DP600, and DP980 (both AHSS). The HSS and the AHSS have been developed for automotive part manufacturing such as structural, exterior, enclosure, and suspension applications to improve crash and part performance. The nominal thicknesses of the DP600, DP980, and HSLA were 1.2 mm, 1.2 mm, and 1.14 mm, respectively and hence a very minor difference in section thickness (approximately 5% variation). The microstructures of the parent metals have been introduced for reference in this work, as shown in Fig. 2. Scanning electron microscopy (SEM) images corresponding to HSLA, DP600, and DP980 are depicted in Figs. 2(*a*)–2(*c*), respectively. Typical α-ferrite matrix for HSLA steel is illustrated in Fig. 2(*a*) in which the grain boundaries are clearly revealed. Characteristic second-phase submicron particles (bright) were randomly distributed within the α-grains. DP600 was composed of a ferrite matrix (α) along with banded islands of martensite (M), which were found to be aligned parallel to the direction of rolling, as observed in Fig. 2(*b*); the volume fraction of the martensite islands on DP600 steel was of approximately 26%. A

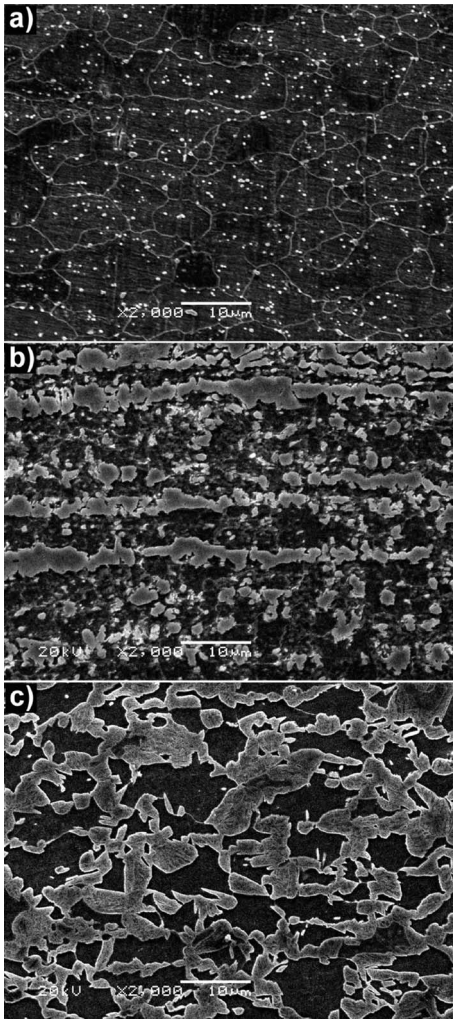

Fig. 2 Base metal microstructure corresponding to (*a*) HSLA, (*b*) DP600, and (*c*) DP980 steel

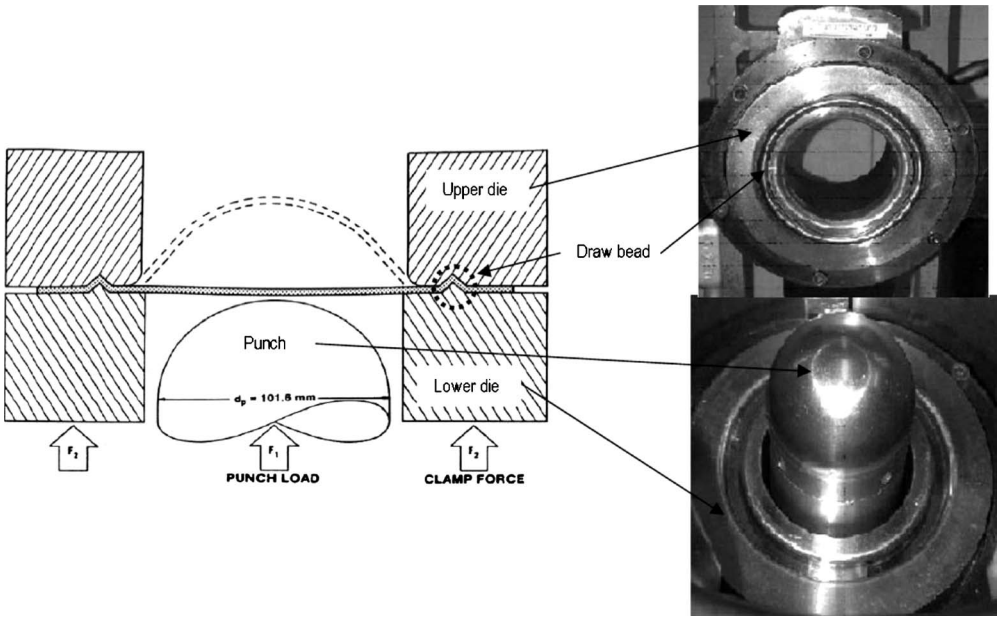

Fig. 3 Arrangement of tools in the experimental set-up for limiting dome height testing

relatively higher volume fraction of martensite phase (i.e., around 54%) resulted on DP980 steel; details of the microstructure are observed in Fig. 2(*c*).

HSLA steel sheets were laser butt welded with DP600 and DP980 steel sheets to produce two dissimilar material combinations (TWBs): DP600-HSLA and DP980-HSLA. The sheets were clamped side by side precisely in a fixture and welded with a 4 kW high power diode laser (HPDL). While welding, the laser beam was aligned with the joint to ensure an equal and consistent amount of melting in both sheets. The laser beam had a rectangular dimension of 12×0.9 mm^2 with a focal length of 80 mm and it was focused at the top corner surface of the thicker sheet to allow the melted metal to join the two sheets. The welding process was carried out in conduction mode with a speed of 1.0 m/min to get full penetration weld without defects such as porosity and cracking [5,11]. In all the welded specimens, the weld line was oriented transverse to the rolling direction of sheets.

3 Mechanical Testing

The various experimental techniques used to characterize the tensile properties of parent materials and TWBs, and to study formability of these welded blanks are discussed in Secs. 3.1 and 3.2.

3.1 Uniaxial Tensile Testing

3.1.1 Parent Material. Uniaxial tensile tests were carried out on parent metal sheets machined as per ASTM standard E8M specification [13]. The tests were conducted along three directions with respect to rolling direction in the sheet (e.g., with tensile axis being parallel (0°), diagonal (45°), and perpendicular (90°) to the rolling direction of the sheet). During the testing, a constant cross head speed of 2 mm/min was employed in all cases. The various tensile properties, such as 0.2% offset yield strength (YS), ultimate tensile strength (UTS), % elongation, strain-hardening coefficient (n), and strength coefficient (K), were determined. The strain-hardening behavior of the sheets was described by using the Hollomon equation [14]. The plastic strain ratio (R) of the parent materials was evaluated using specimens made according to ASTM E517 specification [13]. For determining the R value, specimens were elongated to 75% of the uniform elongation (before reaching the maximum load). Final width and gauge length were measured and the plastic strain ratio (R) was calculated from the following equation [1]. The R value was evaluated in three directions as mentioned in the tensile tests by repeating the above procedure [15].

$$R = \frac{\varepsilon_w}{\varepsilon_t} = \frac{\varepsilon_w}{-(\varepsilon_w + \varepsilon_l)} = \frac{\ln\left(\frac{w_f}{w_0}\right)}{\ln\left(\frac{l_0 \cdot w_0}{l_f \cdot w_f}\right)} \tag{1}$$

where w_0 and l_0 are the initial width and length, w_f and l_f are the final width and length, ε_w is the true width strain, ε_t is the true thickness strain, and ε_l is the true length strain.

3.1.2 Tailor Welded Specimens. Specimens were cut from the laser welded samples for conducting the tensile tests in the transverse direction on the TWBs as per ASTM E8M standard [13]. Transverse tests were used to ensure the weld quality and the weld position whereas varied to understand the effect of weld location on forming behavior during uniaxial tensile deformation.

3.2 Limiting Dome Height Testing

3.2.1 Biaxial-Stretch Forming. LDH tests were done according to the procedure suggested by Hecker [16] using a hemispherical punch of 101.6 mm diameter on a double action MTS hydraulic press to evaluate the formability. Figure 3 shows the schematic diagram of arrangement of tools (punch, lower die, and upper die) used in the stretch forming experiments. A draw bead was fabricated on the dies to clamp the blank rigidly during application of blank holding pressure and to restrict the flow of metal from the flange region into the die opening. Five different square specimens of size 200×200 mm^2 were cut from the laser welded specimens, as shown in Fig. 4, such that weld line was placed at different locations in the TWBs. Two centerlines were marked on the welded specimens by keeping the HSLA sheet on the right side of the TWB. The centerline that was passing parallel to the weld is referred as vertical centerline and the other passing perpendicular to the weld is referred as horizontal centerline. By marking both the centerlines basically helped in two purposes: (a) evaluating the weld locations with respect to vertical centerline and (b) aligning the blank with respect to both centerlines on the die before forming experiment. When the weld is located toward the left of the vertical center line, it is referred to as a $-ve$ weld location, while the weld located on the right of this centerline is

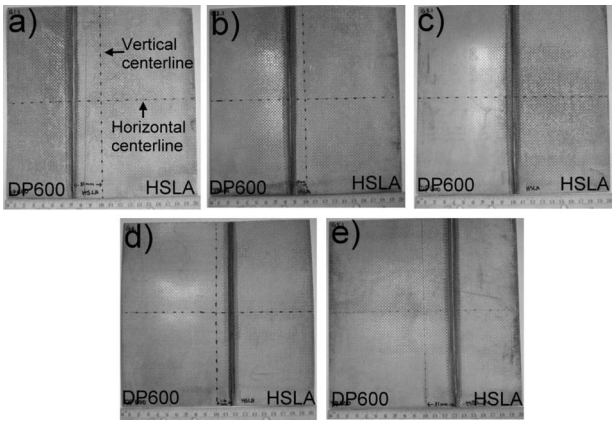

Fig. 4 Laser welded blanks fabricated with different weld locations for biaxial-stretch forming tests: (*a*) −30 mm, (*b*) −15 mm, (*c*) center, (*d*) 15 mm, and (*e*) 30 mm

referred to as *+ve*. The same convention is used in all laser welded blank with different weld locations. The TWB was placed on the lower die so that both the marked centerlines passed the middle of the die opening. An optimum blank holding force was applied to ensure deformation only within the die opening. All these tests were conducted in lubricated condition to induce strain biaxiality during stretch forming at a punch speed of 12 mm/min. The effect of thickness difference can be neglected without using packing strip as there is a very small variation in the thickness among these different sheets. Circular grids of 2.5 mm diameter were marked on the blanks by electrochemical etching technique to measure major and minor strains after deformation. The experiments were stopped when a visible neck or initiation of fracture was observed on the specimens. Figure 5 shows the typical strain distribution pattern for the parent metal (HSLA, DP600, and DP980) obtained from the test and it ensure close to equibiaxial strain state during stretch forming.

3.2.2 Plane Strain Stretch Forming. Plane strain condition refers to when the minor principal strain is zero and it is one of the most common modes of deformation at which failure occurs [17]. After a few trial experiments (without the application of lubrication) by varying the sample width, it was found that a near plane strain condition could be achieved with a sample width of 120 mm. For instance, the strain distribution pattern in domed parts using 120 mm width parent sheet metal (HSLA, DP600, and DP980) is shown in Fig. 6. It is clearly evident from Fig. 6 that the minor strains are close to zero in all cases. So, rectangular TWB blanks of 200×120 mm^2 were used to conduct LDH test in plane strain condition. As shown in Fig. 7, TWBs of both transverse weld direction (weld line was parallel to width and it was referred as transverse laser welded samples) and longitudinal weld direction (weld line was parallel to length and it was referred as longitudinal laser welded samples) were tested. These blanks were deformed by the same 101.6 mm diameter punch until the initiation of fracture with the same optimum blank holding force. In the transverse specimens, the major strain was perpendicular to the weld line. In the longitudinal specimen, the major strain was along the weld line.

All the LDH and tensile tests were carried out using five samples for each condition to observe consistency in results and the average values were reported.

4 Results and Discussion

4.1 Tensile Testing. The standard tensile properties 0.2% offset YS, UTS, % elongation, strain-hardening coefficient (n), strength coefficient (K), and anisotropic parameters (R_0, R_{45}, and R_{90}) of all parent steel sheets determined from the uniaxial tensile

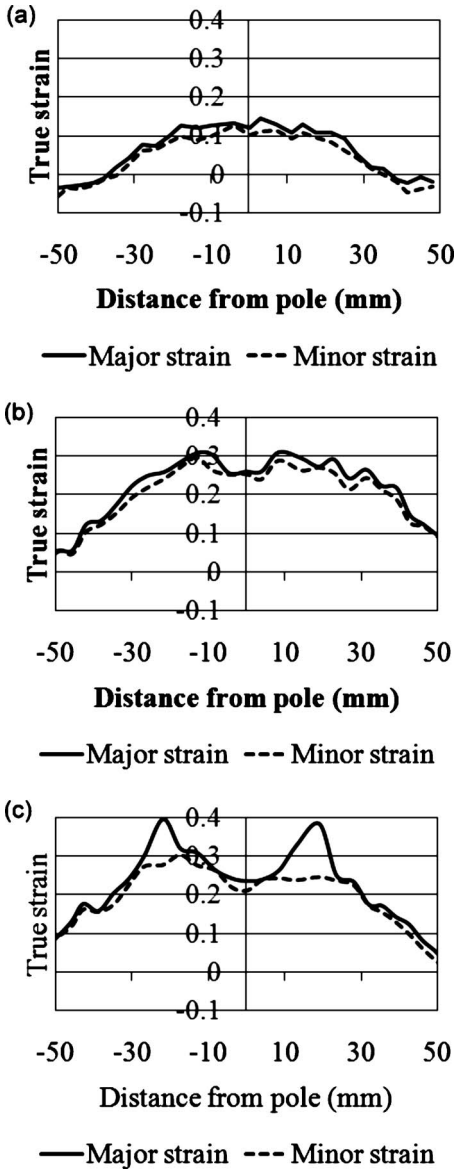

Fig. 5 Major and minor strain distribution on biaxial-stretch formed parent metals: (*a*) DP980, (*b*) DP600, and (*c*) HSLA

tests are given in Table 1. All these steels have different mechanical properties and have potential applications in sheet metal forming due to their higher UTS and ductility.

In all transverse TWB tensile specimens, necking/fracture occurred at HSLA side and the failure location depended on material combination and the weld location. Comparison of engineering stress-engineering strain diagram of the transverse laser welded blank (weld at the middle) with the parent metal is shown in Fig. 8. It was observed that the strength of laser welded blank was comparable to that of HSLA parent material and % elongation decreased as weld line was placed more toward the *+ve* side (Fig. 9). During the tensile deformation of TWBs, there was negligible deformation on the stronger side (DP600 and DP980) and most of the deformation was coming from the weaker HSLA side. This negligible deformation is due to higher UTS and strength coefficient (K) of DP980 and DP600 compared with the HSLA steel sheet. A typical major strain distribution across the weld in deformed DP600-HSLA laser welded samples with different weld locations is shown in Fig. 10. As the weld was placed more toward the *+ve* side in the tensile specimens, less HSLA material was available for deformation and hence % elongation decreased.

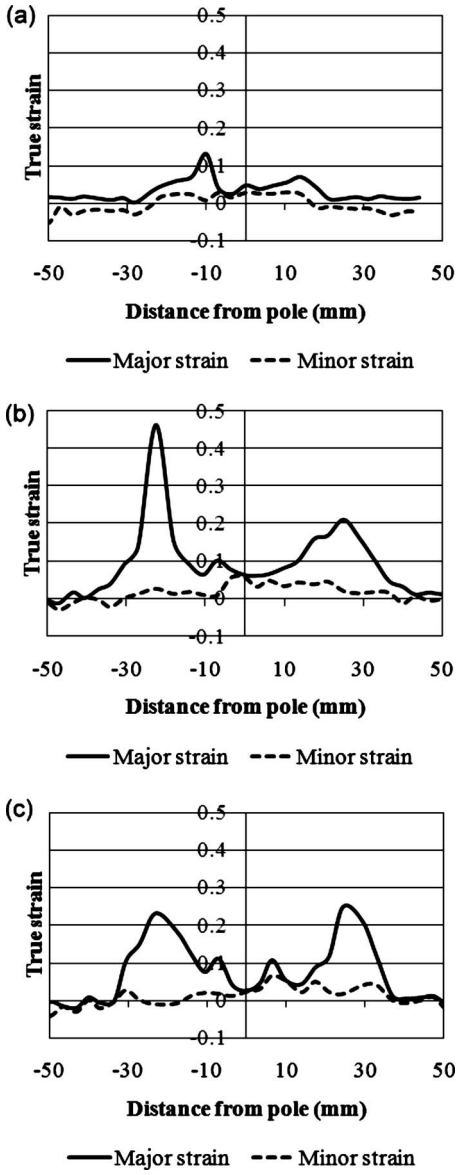

Fig. 6 Major and minor strain distributions on plane strain stretch formed parent metals: (*a*) DP980, (*b*) DP600, and (*c*) HSLA

4.2 Failure Observations

4.2.1 Failure Location

4.2.1.1 Biaxial-stretch forming. The biaxial strain stretch formed samples with different weld locations for DP600-HSLA and DP980-HSLA are shown in Figs. 11 and 12, respectively. The failure location has been pointed out on individual samples. It was found that the failure is on the HSLA side close to weld line (i.e., 3–5 mm) in DP980-HSLA TWBs (Fig. 12(*c*)), but away from the weld line (ranging from 8–15 mm) in DP600-HSLA TWBs (Fig. 11(*c*)) when weld was placed at the center of the blank. The failure location was observed to be very close to the weld when there was larger difference in material properties of either side of the welded blank and hence depended on material combination. It was also observed that failure location depended on the weld position in the biaxial-stretch formed dissimilar laser welded blanks. The failure was also observed consistently located on the HSLA side for all the laser welded blanks when weld was placed at ± 15 mm from the vertical centerline. However, failure shifted to across the weld in both the combinations, DP980-HSLA combination (Fig. 12(*a*)) and in DP600-HSLA combination (Fig. 11(*a*)) when weld was placed at -30 mm.

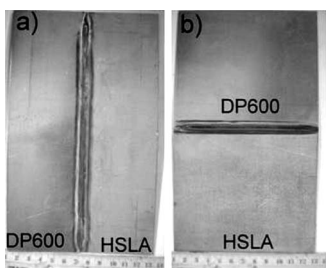

Fig. 7 Laser welded blanks fabricated with different weld orientations for plane strain stretch forming tests: (*a*) longitudinal weld and (*b*) transverse weld

4.2.1.2 Plane strain stretch forming. All the plane strain stretch formed samples with failure location is shown in Fig. 13. In the longitudinal laser welded DP600-HSLA samples, the fracture originated at the fusion zone, as shown in Fig. 13(*a*), whereas fracture was in weaker HSLA sheet in the transverse welded DP600-HSLA samples, as shown in Fig. 13(*b*). Similar failure location was observed in plane strain stretch formed welded DP980-HSLA samples (Figs. 13(*c*) and 13(*d*)). It can be seen on the longitudinal welded samples that the weld line was stretched in the direction of major strain. However, in the transverse welded sample, the weld FZ was at the pole and undergoes less deformation as discussed in Sec. 4.4. Hence, formability of laser welded blank is dominated by difference in properties in transverse welded samples and by weld properties (ductility) in longitudinal welded samples.

4.2.2 Fracture Mode. Figures 14–16 are the representative images for the biaxial stretch formed, the transverse plane strain stretch formed, and the longitudinal plane strain stretch formed specimens, respectively. Each figure shows the (a) the cross section macrostructure at the location of failure, (b) the microstructure beside the failure by optical microscopy, and (c) the fractured surface by SEM imaging.

4.2.2.1 Biaxial-stretch formed specimens. Figure 14(*a*) shows the location of failure at the HSLA sheet few millimeters from the fusion zone, i.e., for dissimilar DP980-HSLA. Observable necking resulted at the location of failure (HSLA) in which a reduction in sheet thickness at the tip was of about 75% (i.e., final thickness was of 0.27 mm beside the tip). Figure 14(*b*) shows the deformed HSLA microstructure just beside the failure (region of necking). At this region, the α-grains appeared elongated and the second-phase particles (dark) seemed aligned toward the prior sheet rolling direction. Cuplike depressions revealed dimple fracture mode, as indicated by the SEM fractograph in Fig. 14(*c*). The dimples appeared equiaxed and uniformly distributed along the fractured surface. Predominant ductile fracture was found on the biaxial strain formed specimens for both dissimilar combinations (DP980-HSLA and DP600-HSLA) possibly initiated at the second-phase particles contained in the HSLA steel sheet [14].

4.2.2.2 Transverse plane strain stretch formed specimens. The macrograph in Fig. 15(*a*) (i.e., DP600-HSLA combination) shows the failure localized at the region of necking on the HSLA side where a thickness reduction of 70% was achieved (i.e., 0.36 mm at the tip). Elongated α-grains and second-phase particles were clearly observed in Fig. 15(*b*). The presence of dimples sparsely distributed along with apparent sheared surface were revealed in Fig. 15(*c*). Even though predominant dimple morphology was revealed at specimens subjected to transverse plane strain forming, the presence of sheared surfaces have indicated a distinct failure mechanism compared with that of the specimens subjected to biaxial strain forming.

Table 1 Tensile properties of various AHSS sheets used in the present study

Steel grade	YS (MPa)	UTS (MPa)	Uniform elongation (%)	Total elongation (%)	n-value	K-value (MPa)	R-value		
							R_0	R_{45}	R_{90}
DP600	365.2	631.4	16.0	25.6	0.21	1097.6	0.80	0.96	1.03
HSLA	421.0	511.2	13.5	25.6	0.13	760.9	1.02	1.23	1.16
DP980	672.3	1058.2	6.9	12.1	0.10	1505.4	0.83	0.91	1.05

4.2.2.3 Longitudinal plane strain stretch formed specimens. Failure was found in the FZ of the specimens tested under longitudinal plane strain forming, as shown by Figs. 16(*a*) and 16(*b*). Observations made on the macrostructure did not reveal any apparent necking (Fig. 16(*a*)). The fracture seemed to propagate upon a 45 deg path with respect to the sheet surface. Failure was apparently initiated in the FZ and extended first through the HAZ and in a later stage toward base metal (BM) (Figs. 13(*a*) and 13(*c*)). The FZ microstructure beside the failure revealed to be composed mainly of martensite, some bainite phase, and certain volume fractions of side plate structures (allotriomorphs ferrite), as shown by Fig. 16(*b*) (DP600-HSLA combination). The fracture surface at the fusion zone shown in Fig. 16(*c*) revealed scarcely shallow dimples and a large number *trans*-granular cleavage shaped fractured regions [18]. *Trans*-granular fracture was also confirmed by observing at the edge of fracture in Fig. 16(*b*).

From the above mentioned observations it is possible to infer that the fracture mode of these stretch formed TWB specimens is highly dependent on the weld orientation as well as the state of strain (biaxial or plane strain) imposed during the different forming test configurations.

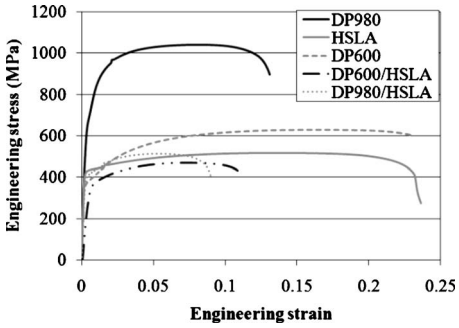

Fig. 8 Engineering stress-engineering strain curves of parent metals and transverse laser welded blanks

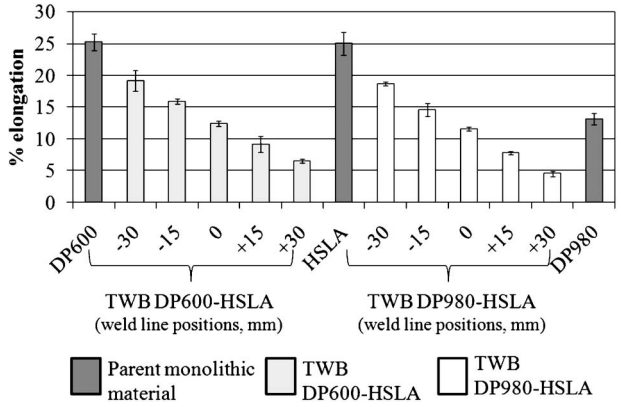

Fig. 9 Percentage elongation obtained from uniaxial tensile testing of transverse laser welded blanks for different weld locations

4.3 Limiting Dome Height

4.3.1 Effect of Material Properties and Weld Location. The comparison of LDH obtained in biaxial-stretch forming is shown in Fig. 17. All the welded samples had lower LDH compared with both the parent metals. This was due to the presence of weld zone and difference in material properties within the blank, which induced nonuniform deformation. The larger the differences in properties between the parent materials, the lower the formability of the TWB due to higher nonuniformity in the deformation during stretch forming. Hence, the LDH of DP980-HSLA was lower than that of DP600-HSLA combination. As shown in Fig. 17, the LDH for DP600-HSLA combination was lower (23–24 mm) when the weld was located −15 mm, 0 mm, and +15 mm from the vertical center line and it increased by 27–33% when the weld

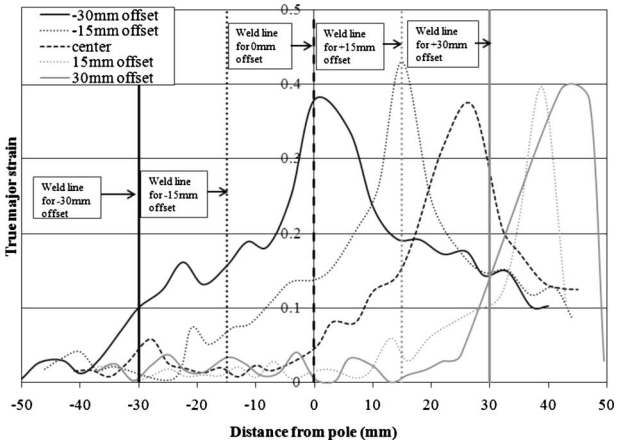

Fig. 10 Major strain distribution across the weld of transverse laser welded (DP980-HSLA) uniaxial tensile specimens for different weld locations

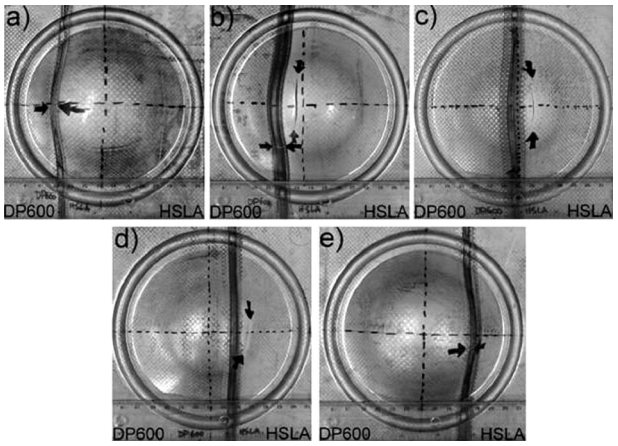

Fig. 11 Biaxial-stretch formed DP600-HSLA laser welded coupons with different weld locations from center: (*a*) −30 mm, (*b*) −15 mm, (*c*) center, (*d*) 15 mm, and (*e*) 30 mm

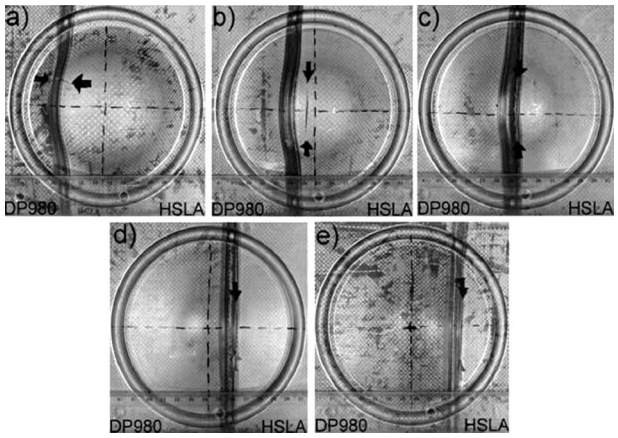

Fig. 12 Biaxial-stretch formed DP980-HSLA laser welded coupons with different weld locations from center: (*a*) −30 mm, (*b*) −15 mm, (*c*) center, (*d*) 15 mm, and (*e*) 30 mm.

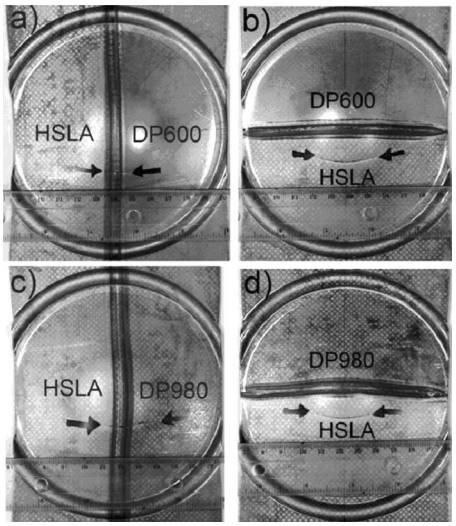

Fig. 13 Plane strain stretch formed laser welded coupons with different weld orientations: (*a*) longitudinal DP600-HSLA, (*b*) transverse DP600-HSLA, (*c*) longitudinal DP980-HSLA, and (*d*) transverse DP980-HSLA

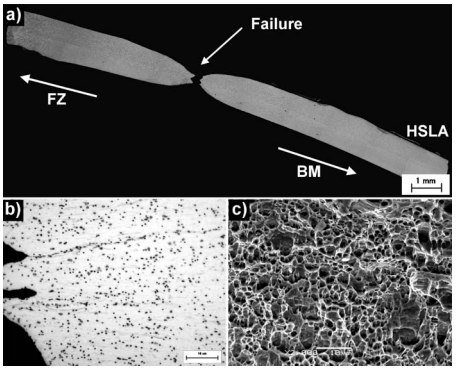

Fig. 14 Representative images of the biaxial stretch forming specimen showing (*a*) cross section macrostructure at the location of failure, (*b*) microstructure beside the failure, and (*c*) fractured surface

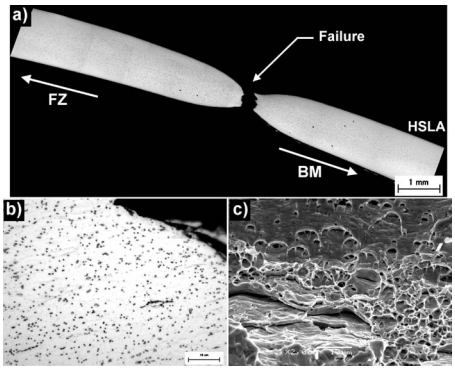

Fig. 15 Representative images of the transverse plane strain forming specimen showing (*a*) cross section macrostructure at the location of failure, (*b*) microstructure beside the failure, and (*c*) fractured surface

was placed at ±30.0 mm away from the vertical center line. Similarly, for the DP980-HSLA combination, the LDH was lower when the weld was located at +15 mm from the vertical center line and it increased by (147.7%) when the weld was placed at −30 mm away from the vertical center line. This increase indicates that there is a significant influence of weld location in stretch forming of dissimilar laser welded blank and the formability can be increased by keeping the weld line away from the pole. However, the level of increase in formability with respect to weld position (either toward the +*ve* side or the −*ve* side) depends on the material combination. Figure 18 shows a comparison of load

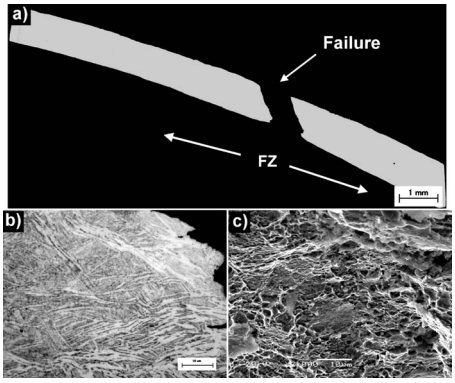

Fig. 16 Representative images of the longitudinal plane strain forming specimen showing (*a*) cross section macrostructure at the location of failure, (*b*) microstructure beside the failure, and (*c*) fractured surface

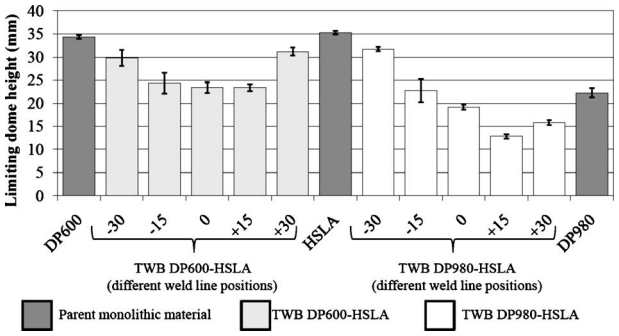

Fig. 17 Comparison of limiting dome height of laser welded blanks with different weld positions during biaxial-stretch forming

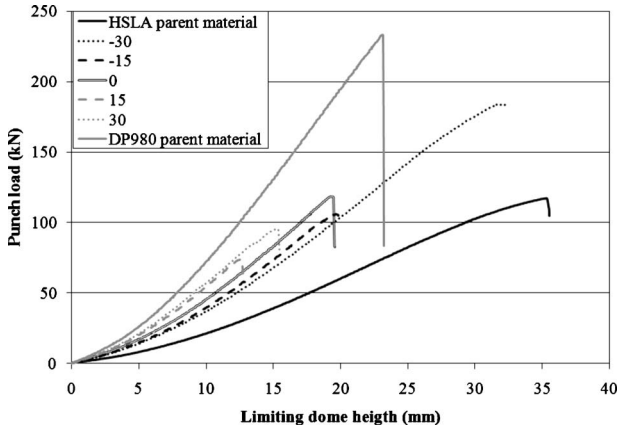

Fig. 18 Comparison of load progression curves obtained during biaxial-stretch forming of DP980-HSLA laser welded blanks with the parent metals

progression during biaxial-stretch forming of DP980-HSLA laser welded blanks with different weld locations. It was found that the load progression curve for a laser welded blank lies within the parent metal (DP980 and HSLA) load progression curves and the slope of the curve depended on the amount of HSLA/DP980 in the laser welded blank. However, the peak load depended on the slope of the curve and the dome height achieved. It was observed that the percentage of elongation from uniaxial tensile test (Fig. 9) did not reflect the same trend as that of LDH for laser welded blanks with different weld locations (Fig. 17). Hence, uniaxial tensile test could not predict the actual press performance of laser welded blanks. In previous finding [19], it was well known that formability decreases in deep drawing as the weld line was placed away from the center. The strain distribution profile has been discussed well in Sec. 4.3.2 where the effect of weld placement on formability was clearly well correlated.

4.3.2 Effect of Weld Orientation and Strain Path (Strain Ratio). Figure 19 shows the LDH obtained in plane strain stretch forming. Comparison of welded blank and parent metal was done here. It was found that all the LDH in plane strain condition is lower compared with the biaxial strain stretch formed samples. This is due to the lower forming limit during plane strain condition [20], which induces different fracture morphology (as shown in Figs. 15(*c*) and 16(*c*)) compared with biaxial strain stretch forming mode (Fig. 14(*c*)). The welded blanks have lower LDH compared with the parent metal due to presence of weld and difference in material properties. There was negligible difference in LDH (1.54%) between the longitudinal and transverse specimens for DP600-HSLA laser welded blank combinations; hence, weld

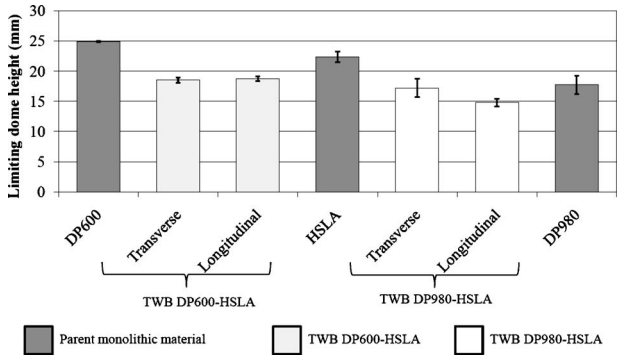

Fig. 19 Limiting dome height of laser welded blanks with different weld orientations during plane strain stretch forming

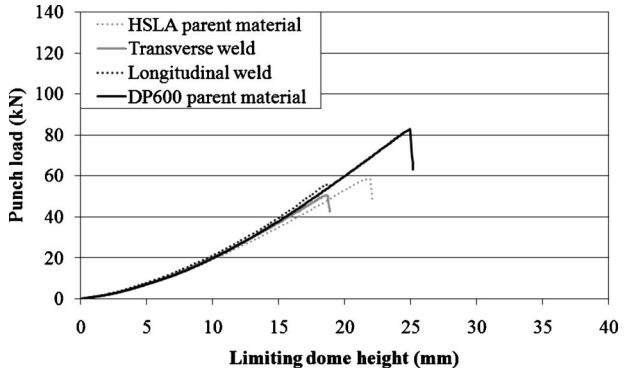

Fig. 20 Load progression curve for DP600-HSLA laser welded blanks obtained during plane strain stretch forming

orientation does not play a significant role compared with the weld location on formability of this dissimilar TWB. This was possibly due to same level of influence of weld zone (in longitudinal laser welded blank) as that of difference in material properties (in transverse laser welded blank) on formability of DP600-HSLA combination, which is also reflected in the load progression curve, as shown in Fig. 20. However, there was significant difference in LDH (16.2%) between longitudinal and transverse welded specimens during plane strain stretch forming of DP980-HSLA combination and it was also found that lower LDH with lower load bearing capacity was observed for the longitudinal welded samples. It was clearly evident that weld orientation had a significant influence on formability of DP980-HSLA welded blanks and that the decrease in formability due to weld zone (in longitudinal welded sample) is larger compared with the difference in properties (in the transverse welded sample). Hence, weld should be oriented transverse to the stretching direction for DP980-HSLA combination in a TWB component design.

4.4 Strain Distribution. The major and minor strain distributions on the dome were plotted with respect to distance from the pole.

4.4.1 Biaxial-Stretch Forming. The major and minor strain distribution patterns across the weld on the deformed TWBs were shown in Fig. 21 for three different weld locations (+15 mm, +30 mm, and −30 mm). In both TWBs cases (i.e., DP600-HSLA and DP980 HSLA), nonuniform strain distribution was observed when weld was located at +15 mm from the center (Figs. 21(*a*) and 21(*b*)). The HSLA side (weaker side) deformed more compared with DP side (either DP600 or DP980, which is the stronger side) during stretch forming of both the laser welded blank and the peak major strain (indicating failure location) was found on HSLA side. Similar type of nonuniform strain distribution pattern was observed on the deformed laser welded blanks when the weld line was located at −15 mm and at center of the blank. All these strain distribution profiles are unlike the strain distribution profile obtained for parent monolithic metal (Figs. 5 and 6) where uniform strain distribution was achieved. However, the major strains were distributed uniformly and the minor strains were also well developed indicating strain path more toward equibiaxial during stretch forming for the deformed laser welded sample when the weld was placed at −30 mm from the center of the blank, as shown in Figs. 21(*c*) and 21(*d*). Hence, the LDH was higher when weld was located at −30 mm from the center of the blank. When the weld was located at +30 mm from the center of the TWB, uniform major strain distribution with well developed minor strain was observed in DP600-HSLA combination (Fig. 21(*e*)) but nonuniform major strain distribution (higher strain and peak on HSLA side) with lower level of minor strain (less than 0.1) was observed in DP980-HSLA combination (Fig. 21(*f*)). When the weld was placed at +30 mm in the DP980-HSLA combination,

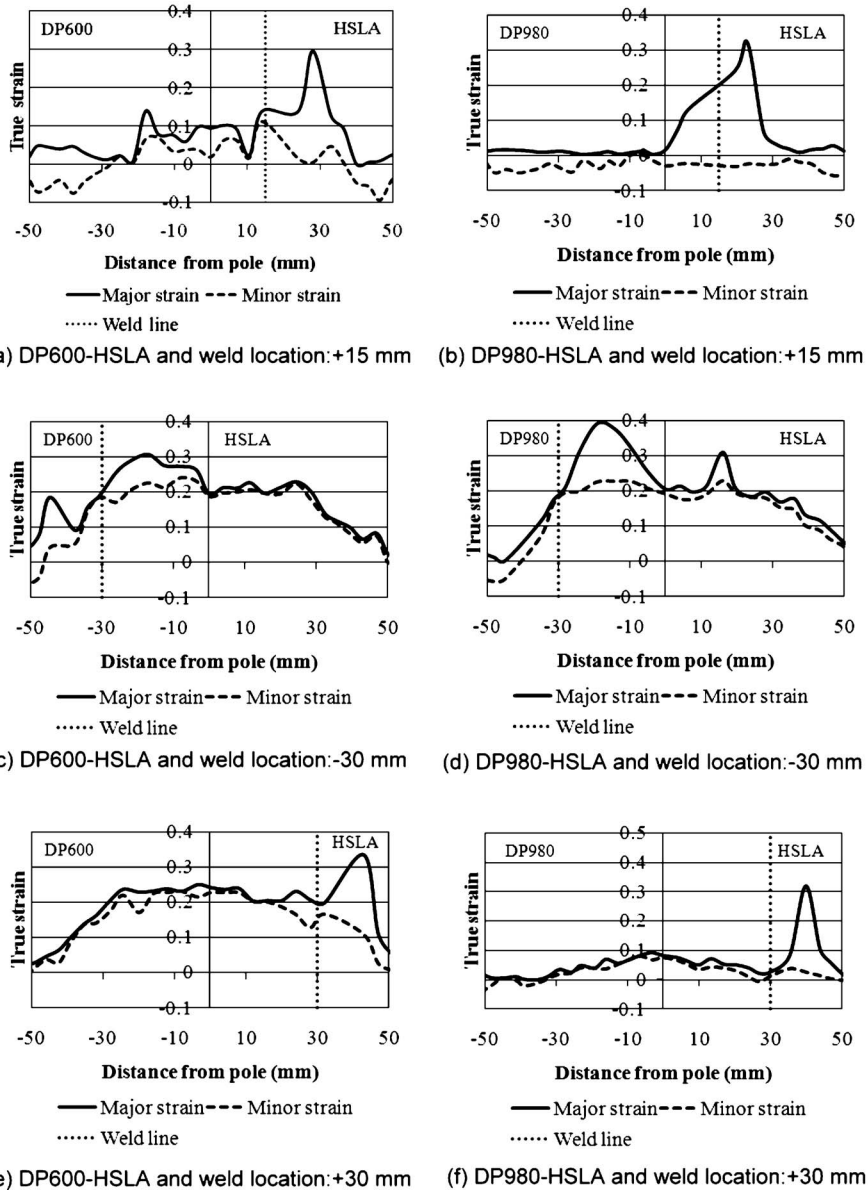

Fig. 21 Major and minor strain distribution patterns for biaxial-stretch formed DP600-HSLA and DP980-HSLA laser welded blanks at three different weld locations

the DP980 side dominates more over the HSLA side by stretching the weaker HSLA side during forming as there was higher amount of DP980 material compared with HSLA material and these two steel have significant difference in properties (unlike DP600 and HSLA). Hence, strain distribution and LDH of dissimilar material combination depends on both weld position and the difference in material properties on either side of the blank. If there is a significant difference in properties between the two materials (such as DP980 and HSLA) while fabricating TWBs, it is desirable to have a lower amount of the stronger material in the component for achieving higher formability in the welded blank.

4.4.2 Plane Strain Stretch Forming. Strain distributions of deformed 120 mm width longitudinal and transverse laser welded samples of DP600-HSLA and DP980-HSLA combination are shown in Fig. 22. In all these samples, it can be observed that the minor strains are close to zero (as the case of parent metals in (Fig. 6)), which indicates that plane strain condition is almost achieved during stretch forming of 120 mm width TWBs. Figure 22(*a*) shows the strain distribution pattern along the weld line in longitudinal weld specimen of DP600-HSLA, which shows comparable peak strains (at the point of failure) on both sides, and the distributions on both sides are similar. Very negligible deformation took place at the pole with major strain value close to zero. However, strain distribution on deformed transverse welded specimen of DP600-HSLA (Fig. 22(*b*)) shows that HSLA experienced higher strain (peak strain) compared with DP600 (stronger side). This strain pattern was comparatively the same as that of deformed longitudinal specimen for DP600-HSLA (Figs. 22(*a*) and 22(*b*)) combination and hence, the LDH of the transverse specimens is similar to that of the longitudinal specimens. Comparing the strain distribution between the deformed longitudinal and transverse specimens of DP980-HSLA combination (Figs. 22(*c*) and 22(*d*)), only one peak was observed in the longitudinal samples with negligible strain elsewhere along the weld and higher strain levels were observed in the transverse specimen due to another peak at the DP980 side. Hence, transverse specimens had higher LDH compared with longitudinal specimens in the

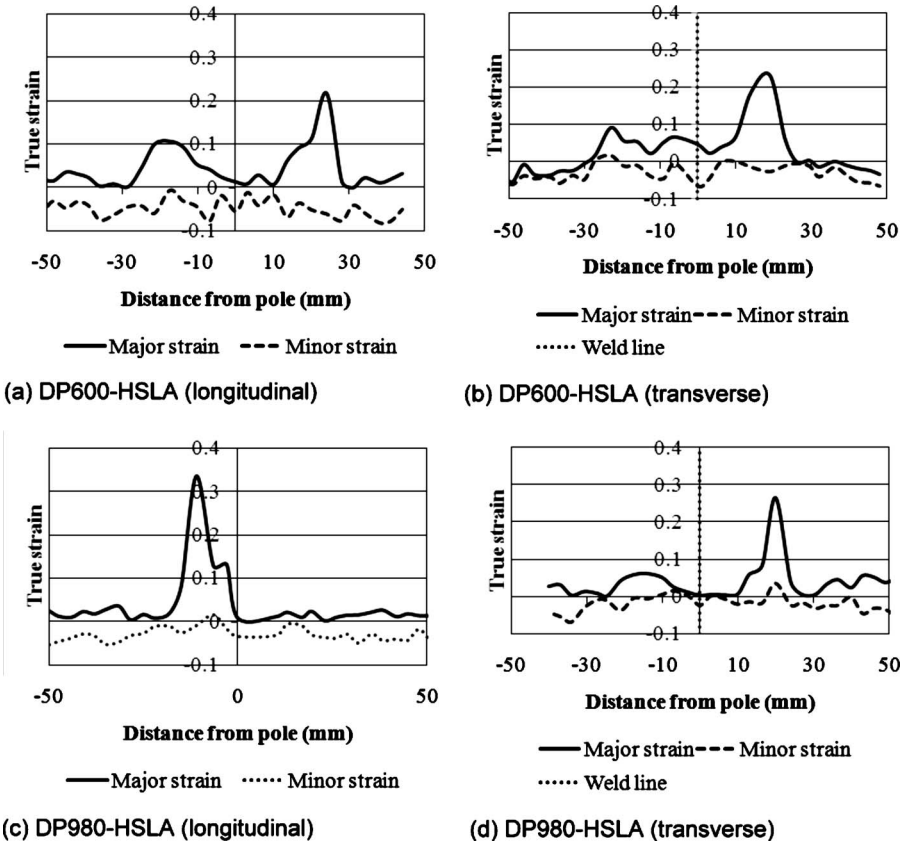

Fig. 22 Major and minor strain distribution patterns for plane strain stretch formed DP600-HSLA and DP980-HSLA laser welded blanks with longitudinal and transverse weld orientations

case of DP980-HSLA combination, indicating influence of weld orientation.

5 Conclusions

The current study investigated the formability of tailor welded blank of advanced high strength steels in terms of LDH during stretch forming. The effects of weld location, weld orientation, and strain path on formability were studied and the followings are the major conclusions.

1. Formability in terms of LDH for dissimilar material laser welded blanks depends on weld location during stretch forming. When the weld is located close to the center of the blank (± 15 mm), the LDH is at the lowest. However, formability increases when the weld line is moved away from the center. The increase in formability with weld locations depends on the type of materials combinations.
2. Nonuniform strain distribution is the main reason for a decrease in LDH of laser welded blanks compared with parent metal. However, uniform strain distribution on the dome surface can be achieved by placing the weld away from the center and hence formability increases.
3. LDH for laser welded blank decreases during plane strain stretch forming compared with the biaxial-stretch forming. During plane strain stretch forming, fracture morphology changes to sheared surfaces with dimple morphology or *trans*-granular cleavage shaped depending on weld orientation. However, predominant ductile fracture with equiaxed dimples is observed during biaxial-stretch forming.
4. Weld orientation with respect to major strain direction does not influence the formability of DP600-HSLA; however, it has strong influence in DP980-HSLA laser welded blank. This is due to change in the strain distribution pattern by influence of weld and material combinations.
5. Formability of dissimilar laser welded blanks of advanced high strength steels can be increased by manipulating the weld location and orientation in the tailor welded blank part design and strain path during stretch forming process. However, increase in formability also depended on type of material combinations.

References

[1] Auto/Steel Partnership, 1995, "Tailor Welded Blank Design and Manufacturing Manual," Technical Report (http://www.a-sp.org/publication.htm).
[2] International Iron and Steel Institute, 2006, "Advanced High Strength Steel Application Guidelines," www.worldautosteel.org
[3] Mellor, P. B., 1981, "Sheet Metal Forming," Int. Metall. Rev., **1**, pp. 1–20.
[4] Sreenivasan, N., Xia, M., Lawson, S., and Zhou, Y., 2008, "Effects of Laser Welding on Formability of DP980 Steel," ASME J. Eng. Mater. Technol., **130**, p. 041004.
[5] Xia, M., Sreenivasan, N., Lawson, S., and Zhou, Y., 2007, "A Comparative Study of Formability of Diode Laser Welds in DP980 and HSLA Steels," ASME J. Eng. Mater. Technol., **129**, pp. 446–452.
[6] Dry, D., Waddell, W., and Owen, D. R. J., 2002, "Determination of Laser Weld Properties for Finite Element Analysis of Laser Welded Tailored Blanks," Sci. Technol. Weld. Joining, **7**, pp. 11–18.
[7] Panda, S. K., Ravi Kumar, D., Kumar, H., and Nath, A. K., 2007, "Characterization of Tensile Properties of Tailor Welded IF Steel Sheets and Their Formability in Stretch Forming," J. Mater. Process. Technol., **183**, pp. 321–332.
[8] Chan, L. C., Chan, S. M., Cheng, C. H., and Lee, T. C., 2005, "Formability and Weld Zone Analysis of Tailor-Welded Blanks for Various Thickness Ratios," ASME J. Eng. Mater. Technol., **127**, pp. 179–185.
[9] Kalpakjian, S., and Schmid, S. R., 2003, *Manufacturing Engineering and Technology*, Pearson Education, India.
[10] Sreenivasan, N., Kuntz, M., and Zhou, Y., 2007, International Conference on Materials Science Technology. (MS&T) Automotive, Detroit, MI, Sept. 16–20, pp. 267–280.
[11] Baltazar Hernandez, V. H., Panda, S. K., Okita, Y., and Zhou, Y., 2009, "A Study on Heat Affected Zone Softening in Resistance Spot Welded Dual Phase

Steel by Nanoindentation," J. Mater. Sci., **45**, pp. 1365–1383.
[12] Panda, S. K., Baltazar Hernandez, V. H., Kuntz, M., and Zhou, Y., 2009, "Formability Analysis of Diode-Laser-Welded Tailored Blanks of Advanced High-Strength Steel Sheets," Metall. Mater. Trans. A, **40**, pp. 1955–1967.
[13] ASTM Standards, 1999, "Metals Test Methods and Analytical Procedures," Annual Book of ASTM Standards 03.01, pp. 78–98, 501–508.
[14] Dieter, G. E., 1996, *Mechanical Metallurgy*, 3rd ed., McGraw-Hill, New York.
[15] Hosford, W. F., and Caddell, R. M., 1993, *Metal Forming: Mechanics and Metallurgy*, Prentice-Hall, Englewood Cliffs, NJ.
[16] Hecker, S. S., 1974, "A Cup Test for Assessing Stretchability," Met. Eng. Q., **14**, pp. 30–36.
[17] Ghosh, A. K., and Hecker, S. S., 1975, "Failure in Thin Sheets Stretched over Rigid Punches," Metall. Trans. A, **6**, pp. 1065–1073.
[18] 2010, Online ASM Handbook on Fractography, Vol. 12, accessed Jan. 3, http://products.asminternational.org/hbk/index.jsp
[19] Heo, Y., Choi, Y., Kim, H., and Seo, D., 2001, "Characteristics of Weld Line Movements for Deep Drawing With Drawbeads of Tailor-Welded Blanks," J. Mater. Process. Technol., **111**, pp. 164–169.
[20] Hecker, S. S., 1975, "Simple Technique for Determining Forming Limit Curves," Sheet Metal Industries, **52**, pp. 671–675.